Metabolite and transcriptome analyses provide new insights into the generation of the blue supramolecular pigment in cornflower

Chengyan Deng
Beijing Forestry university
Jiaying Wang
Beijing Forestry University
Chenfei Lu
Beijing Forestry University
Yanfei Li
Beijing Forestry University
Yan Hong
Beijing Forestry University
Silan Dai (silandai@sina.com)
Beijing Forestry University

Research article

Keywords: cornflower, blue supramolecular pigment, transcriptome, flavonoid, metal ion

Posted Date: November 7th, 2019

DOI: https://doi.org/10.21203/rs.2.16887/v1

Abstract

Background Generally, cyanidin facilitates pink to red petal colours, whereas it causes the expression of a vivid blue colour in cornflower. Previous chemical studies show that the pure blue colour in cornflower petals originates from a blue supramolecular pigment composed of cyanidins, apigenins and metal ions in a stoichiometric ratio, suggesting that the generation of this blue pigment complex is precisely regulated. However, the potential molecular mechanism remains unclear, restricting the innovation of blue cultivars in flowers originally accumulating cyanidin derivatives.

Results In the present study, we traced the dynamic changes in petal colour from white to violet and, finally, to blue on the same petal in cornflower. Pigment analysis showed that apigenin biosynthesis started in the white region and peaked in the violet and blue regions, while cyanidin accumulated in the blue region to almost 2.5-fold higher than that in the violet region, suggesting that the content ratio of the two flavonoids plays a key role in blue colour development. Nine libraries from the above three colour regions were constructed for RNA-Seq, and 105,506 unigenes were obtained by de novo assembly. The differentially expressed genes among the three colour regions were significantly enriched in the phenylpropanoid biosynthesis and flavonoid biosynthesis pathways, leading to the excavation and analysis of 46 structural genes. Moreover, the R2R3-MYB and IIIf bHLH proteins were identified as cyanidin biosynthetic activators by both the dual luciferase reporter assay and transient over-expression in tobacco leaves. Moreover, eight differentially expressed unigenes possibly involved in metal ion transport, storage, tolerance and chelating processes were screened out.

Conclusion The co-existence as well as the appropriate ratio of cyanidin and apigenin directly influence the blue colour development in cornflower. CcMYB6-1 and CcbHLH1 are identified as activators in regulating cyanidin biosynthesis and metal ion related gene resources that may be involved in chelating with flavonoids are also mined. These obtained results provide new insights into the generation of the blue supramolecular pigment in cornflower.

Background

Flower colour is one of the most attractive traits in ornamental plants, in which blue flowers harvest the consumers' preference for their rare and fantastic sight. Previous studies have illustrated that flavonoids play key roles in the vivid petal colouration, in which anthocyanin is the crucial pigment, while other flavonoids often act as co-pigments [1-3]. The anthocyanin aglycons can be mainly divided into cyanidin, pelargonidin, delphinidin, peonidin, petunidin, malvidin and hirsutidin based on the hydroxylation and methylation patterns of their B-rings. Considering that most natural blue flowers can accumulate delphinidin derivatives in their petals, such as *Delphinium grandiflorum, Gentiana triflora* and *Senecio cruentus* [4, 5], researchers have attempted to rebuild the delphinidin biosynthetic pathway by introducing heterogenous *F3′5′H* and obtained different degrees of blue shift transgenic flowers in *Chrysanthemum × morifolium*, *Rosa hybrida* and *Dianthus caryophyllus* [6-8]. However, this process requires breaking of the original biosynthetic pathway and screening for optimal heterogenous genes, and therefore it is usually

time-consuming and labour-intensive. The cornflower and Himalaya poppy have attracted researchers' great interest for their pure and bright blue petals originating from cyanidin rather than delphinidin [9, 10]. This natural phenomenon indicates that cyanidin derivatives, often known as red pigments, can also generate pure blue colour under specific conditions.

Centaurea cyanus, also known as cornflower, is an annual or biennial herb belonging to the composite family and is widely applied in landscaping and cut flower markets. The mechanism of blue colour development in cornflower has long been a significant research target. Earlier studies have illustrated that the pigment in cornflower results from a metal complex [11, 12]. In 1983, Tamura et al. [13] identified the pigment in blue cornflower as cyanidin-3-*O*-(6"-*O*-succinyl-glucoside)-5-*O*-glucoside (succinylcyanin) and apigenin-4'-*O*-(6-*O*-malonyl-glucoside)-7-*O*-glucuronide (malonylapigenin). The following *in vitro* reconstruction assay provided a blue colour similar to the natural blue petal by mixing succinylcyanin, malonylapigenin, Fe^{3+} and Mg^{2+} at a ratio of 6:6:1:1 [14]. Finally, the blue pigment in cornflower petals was verified as a supramolecular pigment composed of six anthocyanins, six flavones, one Fe^{3+}, one Mg^{2+} and two Ca^{2+} by X-ray crystal structure determination [9]. Thus far, chemists have finally clarified the chemical basis of blue petal pigmentation in cornflower after nearly a century's efforts. However, the potential molecular mechanisms involved in the generation of blue supramolecular remain to be explored.

In 1919, Shibata et al. [15] proposed the metal-complex theory, which noted that metal ions are involved in blue colour development. A follow-up study reported that metal ions could complex with not only cyanidin derivatives but also the delphinidin derivatives, as observed in *Tulipa gesneriana* and *Hydrangea macrophylla*, including mainly Fe^{3+}, Mg^{2+} and Al^{3+} [16, 17]. The biosynthesis of flavonoids occurs on the endoplasmic reticulum, followed by their transport to and deposition in the vacuole [18]. Therefore, the metal ion should also be transported to the vacuole to chelate the flavonoids. Momonoi et al. [19] isolated a vacuolar iron transporter homolog, *TgVit1,* in *T. gesneriana,* and the transient expression experiments revealed that it was responsible for the colour change from purple to blue on the upper petal cells. Based on the same strategy, *CcVIT* was also isolated and found to play a role in transporting the ferrous form into vacuoles by heterologous expression in yeast [20]. However, the concrete function of *CcVIT* still lacks further evidence. In addition, magnesium and calcium ions are also key components in generating the blue supramolecular pigment in cornflower petals according to the X-ray crystal structure [9].

The chemical mechanism of blue cornflower has thus far been clarified, but the potential genetic regulation mechanism involved in the generation of this blue supramolecular pigment remains unclear. In the present study, we traced petal colour development in cornflower, which changed from white to violet and eventually to blue from top to bottom (Fig. 1a). The dynamic changes in pigments and transcriptional genes during petal colour development were detected by ultra-performance liquid chromatography coupled with a photodiode array and tandem mass spectrometry (UPLC-MS/MS) and transcriptome analyses, respectively. The obtained results will provide theoretical guidance for blue flower breeding of ornamental plants based on the cyanidin pathway.

Results

Dynamic changes in petal colour and flavonoid composition in blue cornflower

The pigmentation of cornflower petal occurs from top to bottom gradually. Interestingly, the initial colour was white when petals were embedded in the bracts, and then it changed to violet and finally be pure blue colour, while the three different colour regions coexisted in S2 (Fig. 1a). Quantitative description results showed significant differences among these colour regions on the same petal, with decreasing L^* as well as increasing a^*, $|b^*|$ and C^* during colour development (Fig. 1b). UPLC-MS/MS was performed to detect the flavonoid profiling changes both qualitatively and quantitatively. In total, five flavonoids were isolated, including the detection of two anthocyanidin derivatives at 525 nm (Fig. 1d) and three flavone derivatives at 350 nm (Fig. 1e). Based on the characteristics determined by UV-vis absorption spectroscopy, mass spectrum data (Additional file 1: Table S1) and a previous study [13], peak a1 and a2 were putatively identified as cyanidin-3-*O*-malonyl-glucoside-5-*O*-glucoside (Cy3malonylG5G) and cyanidin-3-*O*-(6"-succinyl-glucoside)-5-*O*-glucoside (Cy3succinylG5G), respectively. Peak f1 was putatively assigned as luteolin-7-*O*-succinyl-glucoside (Lu7succinylG), while peak f2 and f3 sharing the same mass spectrum were identified as mutual isomers, namely apigenin-4'-*O*-(6"-*O*-malonyl-glucoside)-7-*O*-glucuronide (Ap4'malonylG7Gn) (Additional file 1: Table S1) [13]. The quantitative analysis suggested that cyanidin accumulation started in the violet region and reached a maximum in the blue region by as high as 2.5-fold. Moreover, apigenin was initially produced in the white region and reached the highest level in the remaining two colour regions (Fig. 1c). The chemical structure formulas of the main accumulated flavonoids are also shown (Fig. 1f). These results revealed that the blue supramolecular complex in cornflower was generated in a gradual and stoichiometric way, namely, the co-existence of cyanidin and apigenin derivatives as well as their relative ratio were both essential in blue colour development.

Transcriptomic changes during petal colour development

To further explore the molecular mechanisms underlying blue colour development, transcriptome results were obtained from three colour regions (white, violet and blue) on the same petal in S2 with three biological replicates (Fig. 1a). A total of 91.74 G clean bases were obtained with a Q30 base percentage greater than 93%, and short reads were assembled into 105,506 unigenes with a mean length of 1260 bp, suggesting that the sequencing quality was sufficiently high to ensure further analysis (Additional file 2: Table S2). Gene expression was analysed by fragments per kilobase of transcript per million mapped reads (FPKM), and differentially expressed genes (DEGs) were identified among the three colour regions. In comparison to the white region, there were 10,296 and 5,249 DEGs in the blue vs white and violet vs white comparisons, respectively, while the DEGs decreased to 1,601 between the blue vs violet comparison (Fig. 2). This distribution of DEGs suggested that the adjoining colour regions possessed relatively similar life processes and metabolic activities. The GO enrichment analysis indicated that these three comparisons produced similar representations of GO terms that were abundantly enriched in the

metabolic process (GO:0008152), single-organism metabolic process (GO:0044710) and oxidation-reduction process (GO:0055114) within the biological process, in the external encapsulating structure (GO:0030312), cell wall (GO:0005618) and fatty acid synthase complex (GO:0005835) within the cellular component, as well as in the catalytic activity (GO:0003824), transferase activity (GO:0016740) and oxidoreductase activity (GO:0016491) within the molecular function under the corrected p-value $<10^{-4}$ (Additional file 3: Fig. S1; Additional file 4: Table S3). The KEGG pathways, including phenylpropanoid biosynthesis (ko00940) and flavonoid biosynthesis (ko00941), were both significantly enriched in three comparisons. Moreover, starch and sucrose metabolism (ko00500) were the most abundantly enriched pathways when comparing the blue and violet regions to the white region (Additional file 3: Fig. S1; Additional file 5: Table S4). These results provide a global view on the potential life processes and metabolic activities during blue colour development.

Expression patterns of flavonoid biosynthetic genes during petal colour development

Combining the UPLC-MS/MS and transcriptome results, the pigment components and related metabolism played important roles in blue colour development, thereby leading to the excavation of structural genes involved in flavonoid biosynthesis in the combined functional annotations. A total of 46 unigenes were selected as the study focus (Additional file 6: Table S5). Subsequently, the transcriptional profiles showed that the key unigene involved in flavone biosynthesis, *FNS*, was expressed the highest level in the white region and decreased gradually along with further petal colour development to violet and blue colours (Fig. 3a-b). In contrast, the anthocyanin generation genes, including both early biosynthetic genes (*F3H, F3'H*) and late ones (*DFR, ANS, GT, AT*), showed the highest expression peak in the violet region (Fig. 3a&c). These results suggested that the highest gene expression peaks of apigenin and cyanidin biosynthesis occurred earlier than their accumulation peak. To further verify the credibility of the transcriptome data, eighteen DEGs were subjected to qRT-PCR, and the correlation coefficient between them was as high as 0.82, suggesting that the transcriptome was reliable (Fig. 3d).

TFs involved in flavonoid biosynthesis in cornflower

The above results indicated that flavonoid accumulation and gene expression occurred in a gradual and precise manner, which was potentially regulated by upstream transcription factors (TFs). Thus, we acquired a global view of the MYBs and bHLHs obtained in the transcriptome database to further clarify the regulatory mechanisms. A total of 29 and 126 R2R3-MYBs in cornflower and Arabidopsis, respectively, were used to construct a phylogenetic tree (Fig. 4a). MYBs in Sg4, Sg5, Sg6 and Sg7 have been reported to play important roles in flavonoid biosynthesis [21]. In our study, there were two *CcMYBs* in Sg4 (Cluster 7159.48611 and Cluster-7159.50459, renamed as *CcMYB4-1* and *CcMYB4-2*, respectively) and two *CcMYBs* in Sg6 (Cluster 7159.49786 and Cluster-7159.43444, renamed as *CcMYB6-1* and *CcMYB6-2*, respectively). All four MYBs contained the typical R2 and R3 conserved domains by sequence analysis (Fig. 4c). Additionally, a phylogenetic tree of *bHLHs*, including 19 *CcbHLHs* and 145 *AtbHLHs*, was also constructed using the conserved domains (Fig. 4b). The subfamilies were labelled following the *Arabidopsis* bHLH group nomenclature [22]. Four typical conserved bHLH regions were detected in

cornflower bHLH, namely one basic region, two helix regions and one loop region (Fig. 4d). Based on previous study, bHLH proteins of the □f subgroups (TT8, GL3, EGL3 etc.) can interact with R2R3-MYBs and are involved in flavonoid biosynthesis [22, 23]. Therefore, the unigene of cluster-7159.49153 integrated with □f subclades in *Arabidopsis* was selected as a potential regulator involved in flavonoid biosynthesis and designated *CcbHLH1*. Network interaction analysis has recently been developed as a powerful method to predict gene function. Further, the function of five candidate genes was predicted by using the online software STRING 11.0. All of them were highly homologous to the flavonoid biosynthetic genes in *Arabidopsis*, such as *AtMYB4*, *AtMYB90*, *AtMYB114* and *TT8* (Additional file 7: Fig. S2; Additional file 8: Table S6). Moreover, qRT-PCR analysis showed continuously increased expression levels of five candidate genes with petal colour development from white to violet and finally to blue colour (Fig. 5a).

Identification of TFs regulating cyanidin biosynthesis

In comparison to the violet region, the blue region possessed similar apigenin but accumulated 2.5-fold higher cyanidins, suggesting that an appropriate accumulation of cyanidins played an important role in blue colour development in cornflower, which led to further exploration of the potential regulatory mechanisms. Flavanone-3-hydroxylase (F3H) is the first key enzyme determining the cyanidin flux, and dihydroflavonol 4-reductase (DFR) catalysed the transformation of dihydroquercetin to leucocyanidin, both of which play crucial roles in cyanidin biosynthesis [2]. Therefore, the promoters of *CcF3H* and *CcDFR* were obtained by genome walking technology with a length of 1644 bp and 1510 bp, respectively, to clarify the possible regulatory roles of *CcMYBs* and *CcbHLH1* in cyanidin biosynthesis. The *cis*-elements were widely located in two promoters, such as MYBCORE(CNGTTR), MYBPLANT(MACCWAMC), and MYBPZM(CCWACC) recognized by MYB protein and EBOXBNNAPA(CANNTG) recognized by bHLH protein (Fig. 5b). Furthermore, a dual luciferase assay was conducted to explore the *in vivo* regulatory roles. The results showed that only *CcMYB6-1* was able to trans-activate the *CcF3H* and *CcDFR* promoters compared with the empty vector, with approximately 13-fold and 32-fold induction, respectively, while single *CcMYB6-2*, *CcMYB4-1*, *CcMYB4-2* and *CcbHLH1* were unable to induce any promoter activity (Fig. 5c). MYB and bHLH transcription factors usually form a protein complex to regulate anthocyanin biosynthesis. In the presence of *CcMYB6-1* and *CcbHLH1*, the activity of the *CcF3H* and *CcDFR* promoters was stimulated more than 17-fold and 46-fold, respectively. However, *CcbHLH1* co-expression with *CcMYB6-2*, *CcMYB4-1*, and *CcMYB4-2* was still unable to upregulate the activity of the two promoters (Fig. 5c).

A transient expression assay was further conducted in tobacco leaves to effectively verify the roles of *CcMYBs* and *CcbHLH1* in regulating anthocyanin biosynthesis. *CcMYB6-2*, *CcMYB4-1* and *CcMYB4-2* were unable to induce anthocyanin biosynthesis either alone or co-expressed with *CcbHLH1* (data not shown), which was consistent with the results of dual luciferase assay (Fig. 5c). In contrast, there were visible red spots on tobacco leaves infiltrated with *CcMYB6-1*. Moreover, co-expression of *CcMYB6-1* and *CcbHLH1* triggered a clearly larger red area (Fig. 5d), the anthocyanin content of which was almost five times higher than the level accumulated in tobacco leaves infiltrated with *CcMYB6-1* and SK (Fig. 5e).

This result suggested that *CcMYB6-1* and *CcbHLH1* possessed a positive ability to regulate anthocyanin biosynthesis.

Excavation of metal ion related genes

According to a previous study, the blue supramolecular pigment in cornflower is composed of six anthocyanins, six flavones, one Fe^{3+}, one Mg^{2+} and two Ca^{2+} [9]. Pigments synthesized in the endoplasmic reticulum were further transported into the vacuole to be protected from oxidation and subsequent loss of colour [18]. Therefore, the metal ions should also be transported into the vacuole to chelate flavonoids. We further screened unigenes with different expression levels among the three colour regions in the transcriptome database. A total of eight DEGs potentially involved in metal ion transport, storage, chelation and tolerance were screened out, including one each of ferritin, ferrochelatase, vacuolar iron transporter, and magnesium transporter and two each of metallothionein and metal tolerance protein (Fig. 6a). The expression levels of these genes mostly increased with petal colour development from white to violet and finally to blue. Notably, the expression level of metallothionein was at least 18-fold higher than the other unigenes (Fig. 6b). Pearson's correlation analysis showed that the expression patterns of ferrochelatase, magnesium transporter and metallothionein were significantly correlated with $|b^*|$ ($r>0.9$, $p<0.001^{***}$), an important parameter representing the degree of blue, and the expression levels of ferritin as well as metal tolerance protein also exhibited a strong correlation ($r>0.8$, $p<0.01^{**}$) (Additional file 9: Table S7). The concrete functions of these candidate genes in the generation of blue supramolecular pigment remain to be further explored.

Discussion

Flavonoids allow plants to exhibit vivid petal colours, in which anthocyanin is the crucial pigment and other flavonoids often act as co-pigments. Generally, cyanidin facilitates pink to red colours, such as those observed in chrysanthemum and lily flowers [24, 25], whereas cyanidin expresses vivid blue colours in cornflower [9, 20]. A previous study has shown that blue cornflower petals originated from a supramolecular pigment composed of six anthocyanins, six flavones, one Fe^{3+}, one Mg^{2+} and two Ca^{2+} by X-ray crystal structure determination [9]. This finding inspired us to consider that flowers accumulating cyanidin rather than delphinidin, the common blue pigment, could also develop a pure blue colour under certain conditions, namely the presence of appropriate co-pigment and metal ions. However, the underlying mechanisms involved in the generation of blue supramolecular pigment remains unclear, restricting the innovation of blue cultivars in flowers originally accumulating cyanidin derivatives. In the present study, we traced the dynamic petal colour changes from white to violet and finally to blue in cornflower. The UPLC-MS/MS results showed that the violet and blue region accumulated similar apigenins (Ap), but the content of cyanidins (Cy) in the blue region was 2.5-fold higher than in the violet region, with a Cy/Ap value of 0.32 and 0.14, respectively. This result suggested that the relative content ratio between cyanidin and apigenin played a key role in blue colour development, which was also confirmed in our previous study among mauve, blue and black cornflower cultivars with Cy/Ap of 0.28, 0.63 and 6.63, respectively [26]. In *Dahlia variabilis*, the black cultivar was due to the hyper-accumulation

of cyanidin without flavones, while the mutant of the black cultivar 'Kokucho' recovered the accumulation of flavones and exhibited a purple appearance [27]. When the relative ratio of anthocyanin to flavone was modified by suppressing *FNSII*, a key structural gene converting flavanones to flavones, the flower colour of torenia dramatically changed from blue to pale blue [28]. All these natural cases indicate that the co-existence as well as the appropriate ratio of anthocyanin and flavone directly influence pigmentation.

Based on the significant differences in cyanidin contents among the three colour regions on the same petal, we further explored the potential molecular mechanisms involved in cyanidin biosynthesis. Due to a lack of complete genome information in cornflower, transcriptome sequencing with nine libraries, three each from the white, violet and blue region on the same petal, was conducted to obtain detailed gene information. Finally, a total of 46 structural genes were mined, and the anthocyanin biosynthetic genes showed the highest expressional peak in the violet region (Fig. 3). This finding suggested that the gene expression peak in the violet region took precedence over the anthocyanin accumulation peak in the blue region, in contrast to other reports in chrysanthemum and waterlily showing that both gene expression and anthocyanin accumulation reach their highest peaks at the same stage [29, 30]. To further clarify the potential regulatory mechanisms, four R2R3 *MYB*s and one IIIf *bHLH* were screened out by phylogenetic and sequence analysis (Fig. 4). A conserved motif necessary for interaction with R/B-like bHLH proteins, $[D/E]LX_2[K/R]X_3LX_6LX_3R$, was found in four *CcMYB*s [31]. The two *CcMYB6*s also contained the ANDV motif related to anthocyanin biosynthesis [32]. MYB and bHLH proteins usually generate synergistic effects on anthocyanin biosynthesis [23]. However, tobacco leaves infiltrated with single *CcMYB6-1* can also accumulate spots of anthocyanins, possibly due to the endogenous activity of tobacco *bHLH*, *NtAN1* [33]. When co-infiltrated with *CcMYB6-1* and *CcbHLH1*, both the trans-activity of *CcF3H* and *CcDFR* promoters as well as the anthocyanin content accumulation were significantly enhanced in tobacco leaves (Fig. 5), similar to the cases in chrysanthemum and grape hyacinth [34, 35]. Subgroup 4 of Arabidopsis R2R3 *MYB*s encodes transcriptional repressors, and *AtMYB4* was identified as a repressor in the regulation of phenylpropanoid pathway gene expression [21, 36]. Thus, the two *CcMYB4*s that were highly homologous to *AtMYB4* by STRING analysis (Additional file 7: Fig. S2) were possibly repressors of anthocyanin biosynthesis, which requires further verification. Interestingly, the expression patterns of the two activators increased continuously with colour development rather than being consistent with the expression trend of structural genes, leading to the speculation that they might be involved in other life processes apart from cyanidin biosynthesis, which necessitates further study.

The metal-complex theory was first proposed in the early twentieth century and indicated that blue colour was due to metal complexation by anthocyanin [15]. Subsequently, increasing evidence supporting metal-complex theory was found in multiple blue flowers based on the X-ray crystal structure and *in vitro* reconstruction of flower colour [9, 10, 17, 37, 38]. It is well known that pigments synthesized in the endoplasmic reticulum are further transported and stored in the vacuole [18, 39]. Thus, metal ions should also be transported into the vacuole to chelate flavonoids. The vacuole iron transporter *TgVit1* was first isolated in the ornamental plant *T. gesneriana* and characterized as the key factor changing the original purple colour to blue in transient expression experiments [19]. Further, a dark blue colour similar to the

natural perianth bottom in tulip was obtained by silencing endogenous *TgFER* expression, which encodes an Fe storage protein, in addition to overexpression of *TgVit1* [38]. An amino acid substitution was then found in CcVIT protein of the cornflower purple mutant, resulting in a loss of iron transport activity [20]. Based on the previous study, iron, magnesium and calcium are all important constituents involved in the generation of blue supramolecular pigment in cornflower [9]. Magnesium and calcium are the most abundant divalent cations in plants, and their homeostasis is precisely regulated for optimal growth and development [40]. Iron is an essential micronutrient for plants, and the iron distribution and metabolism are tightly regulated *in vivo* to avoid toxic excess [41]. Therefore, the chelation between metal ions and flavonoids is a precise process that potentially includes metal ion transport, storage, tolerance and chelating. To obtain additional gene resources of metal ion chelation, transcriptomes from the white, violet and blue regions on the same petal were acquired independently. Finally, eight DEGs involved in colour development were screened out, including ferritin, ferrochelatase, vacuolar iron transporter, magnesium transporter, metallothionein and metal tolerance protein, and most of these DEGs showed increased expression with colour development from white to violet and eventually to blue (Fig. 6). Notably, vacuolar iron transported Fe^{2+} to the vacuole, whereas the valence state for chelating flavonoids was Fe^{3+} [9, 20]. These findings suggest that the process of iron oxidation possibly persists after its transport into the vacuole. A previous study has shown that ferritin interact with Fe^{2+} to induce its oxidation and deposition in the central cavity [42], leading to the speculation that the ferritin may play both iron oxidation and storage roles to provide Fe^{3+} chelation with flavonoids during the generation of the blue supramolecular pigment in cornflower, which requires further study. The expression of ferrochelatase in the blue region was almost 30-fold higher than in the white region, which might be involved in the chelation process between metal ions and flavonoids. Interestingly, metallothionein showed expression levels as high as to 4.7×10^4 (FPKM), which was significantly higher than the other DEGs. Plant metallothioneins constitute a family of small Cys-rich proteins that are capable of coordinating metal ions and play important roles in metal tolerance and homeostasis [43, 44]. It remains to be explored whether the metallothioneins are involved in the blue pigmentation in cornflower.

To our knowledge, research on blue petal colour development in cornflower has long been focused on the chemical identification, whereas few gene resources has been well explored, which restricts blue colour innovation based on the cyanidin pathway. In the present study, we combined both metabolic and transcriptome analyses to trace blue colour development in cornflower petals for the first time. To further verify the functions of potential DEGs effectively, virus-induced gene silencing mediated by tobacco rattle virus was attempted in cornflower, and photobleached leaves were obtained by silencing phytoene desaturase. However, the newly grown leaves unfortunately returned to a green colour because the silencing signals could not spread systematically (data not shown). Therefore, further attempts of functional identification are still needed to screen out crucial genes involved in the generation of blue supramolecular pigment in cornflower and to achieve blue colour innovations based on the cyanidin pathway in flowers such as chrysanthemums and lilies.

Conclusions

This study traced the petal colour changes from white to violet and finally to pure blue in cornflower both at metabolic and transcriptional levels. Although possessing similar apigenins, the lower accumulation of cyanidin in the violet region was not sufficient to develop blue colour, suggesting that the content ratio of cyanidin to apigenin played a key role in the generation of blue supramolecular pigment. Further, a transcriptome database from nine libraries was constructed to explore potential molecular mechanisms. The KEGG pathways including phenylpropanoid biosynthesis and flavonoid biosynthesis were both significantly enriched in DEGs from three colour regions. Based on the metabolite and transcriptome differences, 46 structural genes involved in cyanidin and apigenin biosynthesis were further mined and analysed. Moreover, *CcMYB6-1* and *CcbHLH1* were identified as positive activators regulating cyanidin biosynthesis together. Considering that iron, magnesium and calcium are involved in the generation of blue supramolecular pigment, eight DEGs related to the metal ion transport, storage, tolerance and chelating were excavated, four of which were strongly correlated with $|b^*|$, an important parameter representing the degree of blue. Further research is now required to extend insights into the precise regulation of the content ratio between cyanidin and apigenin as well as the molecular mechanisms of metal ion chelation with flavonoids.

Methods

Plant material

The seeds of *Centaurea cyanus* 'Dwarf Tom Pouce Blue' were purchased from the Outsidepride Seed Company and planted in a phytotron at 23 °C, 50% relative humidity and 16-h/8-h (light/dark) culture conditions. The colour development of cornflower petals was divided into four stages similarly to our previous study with a few modifications [26]. Briefly, in S1, the petals were just starting to undergo colouration on the top; in S2, the blue, violet and white regions occupied nearly 25%, 25% and 50% of the whole petal, respectively; in S3, the petals exhibited pure blue colour in all petal regions; in S4, the fully coloured petals opened (Fig. 1a). The visually different colour regions on the same petal in S2 were cut separately with a scalpel, precooled rapidly in liquid nitrogen and stored at -80°C for flavonoid and RNA extraction. Three biological replicates were performed for each colour region.

Measurements of petal colour phenotype and flavonoids

The colourimeter (Avantes AvaSpec-2048 L, Netherlands) were used to describe the colour phenotypes quantitatively. Five random measurements were performed for each sample. For flavonoid profiling analysis of the three colour regions on the same petal, approximately 0.1 g of fresh petal powder was extracted with CH_3CN/H_2O (1:1, v:v) containing 0.5% formic acid [20]. All supernatants were collected and passed through 0.22-μm reinforced nylon membrane filters. Ultra-performance liquid chromatography coupled with a photodiode array and tandem mass spectrometry (UPLC-MS/MS) was used according to our previous study [26]. Standards of cyanidin-*3,5*-di-*O*-glucoside (Cy3G5G) and quercetin 3-*O*-rutinoside (rutin) were used for quantitative analysis. Three biological replicates were performed for each colour region.

RNA extraction, library construction and RNA-Seq

Total RNA was isolated from the three colour regions on the same cornflower petal using the Quick RNA Isolation Kit (Huayueyang Biotechnology Co. Ltd., Beijing, China). The RNA concentration was measured using the Qubit® RNA Assay Kit in a Qubit® 2.0 Flurometer (Life Technologies, CA, USA). RNA integrity was assessed by the RNA Nano 6000 Assay Kit of the Agilent Bioanalyser 2100 system (Agilent Technologies, CA, USA). cDNA library construction and sequencing were performed by Novogene Biotechnology (Beijing, China). mRNA was purified from total RNA using poly-T oligo-attached magnetic beads and broken into short fragments. The first and second-strand cDNAs were synthesized using these broken mRNA fragments as template. After adenylation of the 3' ends of the DNA fragments, NEBNext Adaptor with a hairpin loop structure were ligated to prepare for hybridization. The library fragments were purified with the AMPure XP system (Beckman Coulter, Beverly, USA) to screen cDNAs of 150-200 bp. PCR amplification was performed to enrich the cDNA library. The library quality was assessed on the Agilent Bioanalyser 2100 system. Clustering of the index-coded samples was performed on a cBot Cluster Generation System. After cluster generation, nine libraries were sequenced on an Illumina Hiseq platform, and paired-end reads were generated.

De novo assembly and functional annotation

Raw data reads containing the adapter and poly-N or with low quality were removed to obtain high-quality clean data. Transcriptome assembly was accomplished using Trinity with min_kmer_cov set to 2 by default and all other parameters set to default [45]. Subsequently, the assembled unigenes were annotated using the BLASTx alignment with an E-value $\leq 10^{-5}$ to various protein databases, including the NCBI non-redundant protein sequences (Nr), Protein family (Pfam), Clusters of Orthologous Groups pf proteins (KOG/COG), Swiss-Prot, KEGG Ortholog (KO) and Gene Ontology (GO) databases.

Gene isolation, phylogenetic analysis and amino acid sequence analysis

Full-length mRNA sequences were obtained from the transcriptome directly or were isolated using rapid amplification of cDNA ends (RACE). These sequences were further predicted by Blast search (https://blast.ncbi.nlm.nih.gov/Blast.cgi?PROGRAM=blastx&PAGE_TYPE=BlastSearch&LINK_LOC=blasthome) and translated by EMBOSS getorf (http://emboss.bioinformatics.nl/cgi-bin/emboss/getorf) to obtain full-length protein sequences. A neighbour-joining tree was constructed using MEGA7.0 to analyse the phylogenetic relationship of MYBs or bHLHs between cornflower and *Arabidopsis*. DNAMAN 9.0 software was used to perform multiple sequence alignments of targeted MYB proteins with complete amino acids. Protein sequences were screened against the Pfam database to identify domains in bHLHs. The conserved motif logo of bHLH proteins was generated by WebLogo 3 (http://weblogo.threeplusone.com) [46].

Gene expression analysis

Total RNAs were extracted from three colour regions on the same petal. The cDNA synthesis was conducted according to our previous report [26]. The gene expression patterns were analysed by real-time quantitative reverse transcription polymerase chain reaction (qRT-PCR) following the manufacturer's instructions with SYBR Premix Ex Taq (Takara, Japan). All the primers used in this study are listed (Additional file 10: Table S8). Cornflower actin (KY621346) was used as a reference gene to evaluate the expression patterns of target genes.

Dual-luciferase assays

To verify the regulatory effects of transcription factors on target promoters, the dual luciferase assay was performed. The full-length sequences of *CcMYB*s and *CcbHLH*s were recombined into the pGreenII0029 62-SK vector. The promoter regions of *DFR* and *F3H* were extracted from young leaves of blue cornflower using the Genome Walking Kit (Takara, Japan) following the manufacturer's instructions, further verified using high-fidelity polymerase KOD-Plus-0902 (TOYOBO, Japan) and sequencing . The conserved cis-element motifs located in the promoters were scanned using the online software PLACE (https://www.dna.affrc.go.jp/PLACE/?action=newplace) [47]. The two promoter sequences were cloned into pGreenII 0800-LUC vector, respectively. All the above constructs were individually transformed into *Agrobacterium tumefaciens* GV3101.

GV3101 containing SK-*CcMYB* or/and SK-*CcbHLH* was mixed with the LUC-*CcDFR* or LUC-*CcF3H* promoter at a ratio of 10:1 (v:v) and then infiltrated into tobacco leaves (*Nicotiana benthamiana*) with a needleless injector. Enzyme activities of firefly luciferase and *Renilla* luciferase were detected using the Dual-Luciferase Reporter Assay System (Promega, USA) by EnVision (PerkinElmer, USA).

Transient over-expression assays

Tobacco leaves (*N. tabacum*) were chosen for transient over-expression to screen transcription factors involved in the anthocyanin biosynthesis. GV3101 transformed with SK-*CcMYB*s and SK-*CcbHLH* was infiltrated into tobacco leaves either individually or in combinations at a ratio of 1:1 (v:v). The patches in tobacco leaves were photographed 9 days later, followed by anthocyanin content detection using a previously described method [48].

Statistical analysis

To determine significant differences among samples, Ducan's test was conducted using SPSS 20.0 software (SPSS Inc., Chicago, USA). The correlation relationship between the absolute b^* value and expression of metal ion related genes were calculated and presented in Pearson's correlation coefficient r (Additional file 9: Table S7).

Additional Files

Additional file 1: Table S1. Putative identification of flavonoids in three colour regions of cornflower by I-Class UPLC/Xevo^{TM} TQ MS. (XLSX 17 KB)

Additional file 2: Table S2. Summary of sequencing and assembly quality in RNA-Seq. (XLSX 16 KB)

Additional file 3: Fig. S1. GO (left) and KEGG pathway (right) enrichment analysis for DEGs. (DOCX 1366 KB)

Additional file 4: Table S3. Significantly enriched GO terms in comparisons between different colour regions (P<0.0001). (XLSX 22 KB)

Additional file 5: Table S4. Significantly enriched KEGG pathway in comparisons between different colour regions (P<0.0001). (XLSX 17 KB)

Additional file 6: Table S5. Candidate genes involved in flavonoid biosynthesis in cornflower. (XLSX 18 KB)

Additional file 7: Fig. S2. Interaction network analysis of MYB and bHLH proteins. Line thickness indicates the strength of data support and the interaction score is set as high confidence (0.700). The homologous genes of cornflower and related genes for *Arabidopsis* are marked in blue rectangles. (DOCX 2359 KB)

Additional file 8: Table S6. Annotation summary of proteins involved in the analyses of TFs interaction network. (XLSX 20 KB)

Additional file 9: Table S7. Pearson's correlation analysis comparing gene expression at three colour regions with petal colour phenotype of |b^*|. (XLSX 18 KB)

Additional file 10: Table S8. Primers used in this study. (XLSX 20 KB)

Abbreviations

PAL: Phenylalanine ammonia lyase; 4CL: 4-coumarate: CoA ligase; CHS: Chalcone synthase; CHI: Chalcone isomerase; FNS: Flavone synthase; F3H: Flavanone-3-hydroxylase; F3'H: Flavonoid 3'-hydroxylase; DFR: Dihydroflavonol 4-reductase; ANS: Anthocyanidin synthase; GT: Flavonoid glucosyltransferase; AT: Acyltransferase; UPLC-MS/MS: Ultra-performance liquid chromatography coupled with a photodiode array and tandem mass spectrometry; DEGs: Differentially expressed genes; GO: Gene Ontology; KEGG: Kyoto Encyclopedia of Genes and Genomes; TF: Transcription factor; Cy: Cyanidin; Ap: Apigenin.

Declarations

Acknowledgements

We would like to thank professor Liangsheng Wang at the Chinese Academy of Sciences for his helpful support in conducting the UPLC-MS/MS analysis.

Authors' contribution

SD conceived the study and edited the paper. CD, JW, CL and YL conducted the experiments. CD analysed the obtained data and wrote the manuscript. YH edited the paper. All the authors read and approved the manuscript.

Funding

This research was supported by the National Key Research and Development Program, China (2018YFD1000405).

Availability of data and materials

All data generated or analysed during this study are included in this article and its supplementary information files. RNA-Seq data generated is available with the SRA accession PRJNA577252 in NCBI (http://www.ncbi.nlm.nih.gov/sra).

Ethics approval and consent to participate

Not applicable.

Consent for publication

Not applicable.

Competing interests

The authors declare that they have no competing interests.

Author details

Beijing Key Laboratory of Ornamental Plants Germplasm Innovation & Molecular Breeding, National Engineering Research Center for Floriculture, Beijing Laboratory of Urban and Rural Ecological Environment and College of Landscape Architecture, Beijing Forestry University, Beijing 100083, People's Republic of China.

References

1. Zhang Y, Butelli E, Martin C. Engineering anthocyanin biosynthesis in plants. Curr Opin Plant Biol. 2014;19:81–90.
2. Okitsu N, Noda N, Chandler S, Tanaka Y. Flower Colour and Its Engineering by Genetic Modification. In: Van Huylenbroeck J, editor. Ornamental Crops. Handbook of Plant Breeding. Springer, Cham;

2018. p29–62.

3. Zhao D, Tao J. Recent advances on the development and regulation of flower colour in ornamental plants. Front Plant Sci. 2015; 6:261.
4. Sasaki N, Nakayama T. Achievements and perspectives in biochemistry concerning anthocyanin modification for blue flower colouration. Plant Cell Physiol. 2015;56(1):28–40.
5. Jin X, Huang H, Wang L, Sun Y, Dai S. Transcriptomics and metabolite analysis reveals the molecular mechanism of anthocyanin biosynthesis branch pathway in different *Senecio cruentus* cultivars. Front Plant Sci. 2016;7:1307.
6. Noda N, Yoshioka S, Kishimoto S, Nakayama M, Douzono M, Tanaka Y, Aida R. Generation of blue chrysanthemums by anthocyanin B-ring hydroxylation and glucosylation and its colouration mechanism. Sci Adv. 2017;3:e1602785.
7. Katsumoto Y, Fukuchi-Mizutani M, Fukui Y, Brugliera F, Holton TA, Karan M, Nakamura N, Yonekura-Sakakibara K, Togami J, Pigeaire A, Tao GQ, Nehra NS, Lu CY, Dyson BK, Tsuda S, Ashikari T, Kusumi T, Mason JG, Tanaka Y. Engineering of the rose flavonoid biosynthetic pathway successfully generated blue-hued flowers accumulating delphinidin. Plant Cell Physiol. 2007;48(11):1589–1600.
8. Fukui Y, Tanaka Y, Kusumi T, Iwashita T, Nomoto K. A rationale for the shift in colour towards blue in transgenic carnation flowers expressing the flavonoid 3',5'-hydroxylase gene. Phytochemistry. 2003;63:15–23.
9. Shiono M, Matsugaki N, Takeda K. Structure of the blue cornflower pigment. Nature. 2005;436:791–791.
10. Yoshida, K., Kitahara, S., Ito, D., Kondo, T. Ferric ions involved in the flower colour development of the Himalayan blue poppy, *Meconopsis grandis*. Phytochemistry. 2006;67:992–998.
11. Hayashi K, Saito N, Mitsui S. On the metallic components in newly crystallized specimen of Bayer's protocyanin, a blue metallo-anthocyanin from the cornflower. Proc Jpn Acad. 1961;37:393–397.
12. Asen S, Jurd L. The constitution of a crystalline, blue cornflower pigment. Phytochemistry. 1967;6:577–584.
13. Tamura H, Kondo T, Kato Y, Goto T. Structures of a succinyl anthocyanin and a malonyl flavone, two constituents of the complex blue pigment of cornflower *Centaurea cyanus*. Tetrahedron Lett. 1983;24(51):5749–5752.
14. Kondo T, Ueda M, Tamura H, Yoshida K, Isobe M, Goto T. Composition of protocyanin, a self-assembled supramolecular pigment from the blue cornflower, *Centaurea cyanus*. Angew Chem Int Edit. 1994;33(9):978–979.
15. Shibata K, Shibata Y, Kasiwagi I. Studies on anthocyanins: colour variation in anthocyanins. J Am Chem Soc. 1919;41:208–220.
16. Shoji K, Miki N, Nakajima N, Momonoi K, Kato C, Yoshida K. Perianth bottom-specific blue colour development in Tulip cv. Murasakizuisho requires ferric ions. Plant Cell Physiol. 2007;48(2):243–251.

17. Oyama K, Yamada T, Ito D, Kondo T, Yoshida K. Metal complex pigment involved in the blue sepal colour development of hydrangea. J Agr Food Chem. 2015;63:7630–7635.
18. Bassham DC. Pigments on the move. Nature. 2015;526:644–645.
19. Momonoi K, Yoshida K, Mano S, Takahashi H, Nakamori C, Shoji K, Nitta A, Nishimura M. A vacuolar iron transporter in tulip, TgVit1, is responsible for blue colouration in petal cells through iron accumulation. Plant. J. 2009;59:437–447.
20. Yoshida K, Negishi T. The identification of a vacuolar iron transporter involved in the blue colouration of cornflower petals. Phytochemistry. 2013;94:60–67.
21. Dubos C, Stracke R, Grotewold E, Weisshaar B, Martin C, Lepiniec L. MYB transcription factors in *Arabidopsis*. Trends Plant Sci. 2010;15(10):573–581.
22. Pires N, Dolan L. Origin and diversification of basic-helix-loop-helix proteins in plants. Mol Biol Evol. 2010;27(4):862–874.
23. Xu W, Dubos C, Lepiniec L. Transcriptional control of flavonoid biosynthesis by MYB–bHLH–WDR complexes. Trends Plant Sci. 2015;20(3):176-185.
24. Chen SM, Li CH, Zhu XR, Deng YM, Sun W, Wang LS, Chen FD, Zhang Z. The identification of flavonoids and the expression of genes of anthocyanin biosynthesis in the chrysanthemum flowers. Biol Plantarum. 2012;56(3):458–464.
25. Lai YS, Shimoyamada Y, Nakayama M, Yamagishi M. Pigment accumulation and transcription of *LhMYB12* and anthocyanin biosynthesis genes during flower development in the asiatic hybrid lily (*Lilium* spp.). Plant Sci. 2012;193–194:136–147.
26. Deng C, Li S, Feng C, Hong Y, Huang H, Wang J, Wang L, Dai S. Metabolite and gene expression analysis reveal the molecular mechanism for petal colour variation in six *Centaurea cyanus* cultivars. Plant physiol Bioch. 2019;142:22–33.
27. Deguchi A, Ohno S, Hosokawa M, Tatsuzawa F, Doi M. Endogenous post-transcriptional gene silencing of flavone synthase resulting in high accumulation of anthocyanins in black dahlia cultivars. Planta. 2013;237:1325–1335.
28. Ueyama Y, Suzuki K, Fukuchi-Mizutani M, Fukui Y, Miyazaki K, Ohkawa H, Kusumi T,Tanaka Y. Molecular and biochemical characterization of torenia flavonoid 3'-hydroxylase and flavone synthase and modification of flower colour by modulating the expression of these genes. Plant Sci. 2002;163:253–263.
29. Hong Y, Tang X, Huang H, Zhang Y, Dai S. Transcriptomic analyses reveal species-specific light-induced anthocyanin biosynthesis in chrysanthemum. BMC Genomics. 2015;16:202.
30. Wu Q, Wu J, Li SS, Zhang HJ, Feng CY, Yin DD, Wu RY, Wang LS. Transcriptome sequencing and metabolite analysis for revealing the blue flower formation in waterlily. BMC Genomics. 2016;17:897.
31. Zimmermann IM, Heim MA, Weisshaar B, Uhrig JF. Comprehensive identification of *Arabidopsis thaliana* MYB transcription factors interacting with R/B-like bHLH proteins. Plant J. 2004;40:22–34.

32. Zhai R, Wang Z, Zhang S, Meng G, Song L, Wang Z, Li P, Ma F, Xu L. Two MYB transcription factors regulate flavonoid biosynthesis in pear fruit (*Pyrus bretschneideri* Rehd.). J Exp Bot. 2016;67(5):1275–1284.
33. Montefiori M, Brendolise C, Dare AP, Lin-Wang K, Davies KM, Hellens RP, Allan AC. In the Solanaceae, a hierarchy of bHLHs confer distinct target specificity to the anthocyanin regulatory complex. J Exp Bot. 2015;66(5):1427–1436.
34. Xiang L, Liu X, Li X, Yin X, Grierson D, Li F, Chen K. A novel *bHLH* transcription factor involved in regulating anthocyanin biosynthesis in chrysanthemums (*Chrysanthemum morifolium* Ramat.). Plos One.2015;10(11):e0143892.
35. Chen K, Du L, Liu H, Liu Y. A novel R2R3-MYB from grape hyacinth, MaMybA, which is different from MaAN2, confers intense and magenta anthocyanin pigmentation in tobacco. BMC Plant Biol. 2019;19:390.
36. Hemm MR, Herrmann KM, Chapple C. AtMYB4: a transcription factor general in the battle against UV. Trends Plant Sci. 2001;6(4):135–136.
37. Yoshida K, Tojo K, Mori M, Yamashita K, Kitahara S, Noda M, Uchiyam S. Chemical mechanism of petal colour development of *Nemophila menziesii* by a metalloanthocyanin, nemophilin. Tetrahedron. 2015;71:9123–9130.
38. Shoji K, Momonoi K, Tsuji T. Alternative expression of vacuolar iron transporter and ferritin genes leads to blue/purple colouration of flowers in Tulip cv. 'Murasakizuisho'. Plant Cell Physiol. 2010;51(2):215–224.
39. Zhao J. Flavonoid transport mechanisms: how to go, and with whom. Trends Plant Sci. 2015;20(9):576–585.
40. Tang RJ, Luan S. Regulation of calcium and magnesium homeostasis in plants: from transporters to signaling network. Curr Opin Plant Biol. 2017;39:97–105.
41. Connorton JM, Balk J, Rodríguez-Celma J. Iron homeostasis in plants – a brief overview. Metallomics. 2017;9:813–823.
42. Arosio P, Ingrassia R, Cavadini P. Ferritins: a family of molecules for iron storage, antioxidation and more. BBA-Gen. Subjects. 2009;1790:589–599.
43. Leszczyszyn OI, Imam HT, Blindauer CA. Diversity and distribution of plant metallothioneins: a review of structure, properties and functions. Metallomics. 2013;5(9):1146–1169.
44. Peng JS, Ding G, Meng S, Yi HY, Gong JM. Enhanced metal tolerance correlates with heterotypic variation in SpMTL, a metallothionein-like protein from the hyperaccumulator, *Sedum plumbizincicola*. Plant Cell Environ. 2017;40:1368–1378.
45. Grabherr MG, Haas BJ, Yassour M, Levin JZ, Thompson DA, Amit I, Adiconis X, Fan L, Raychowdhury R, Zeng Q, Chen Z, Mauceli E, Hacohen N, Gnirke A, Rhind N, Palma F, Birren BW, Nusbaum C, Lindblad-Toh K, Friedman N, Regev A. Full-length transcriptome assembly from RNA-Seq data without a reference genome. Nat Biotechnol. 2011;29:644–652.

46. Crooks GE, Hon G, Chandonia JM, Brenner SE. WebLogo: A sequence logo generator. Genome. Res. 2004;14:1188–1190.
47. Higo K, Ugawa Y, Iwamoto M, Korenaga T. Plant cis-acting regulatory dna elements (PLACE) database: 1999. Nucleic Acids Res. 1999;27(1):297–300.
48. Xiang L, Liu X, Li H, Yin X, Grierson D, Li F, Chen K. *CmMYB#7*, an R3 MYB transcription factor, acts as a negative regulator of anthocyanin biosynthesis in chrysanthemum. J Exp Bot. 2019;70(12):3111–3123.

Figures

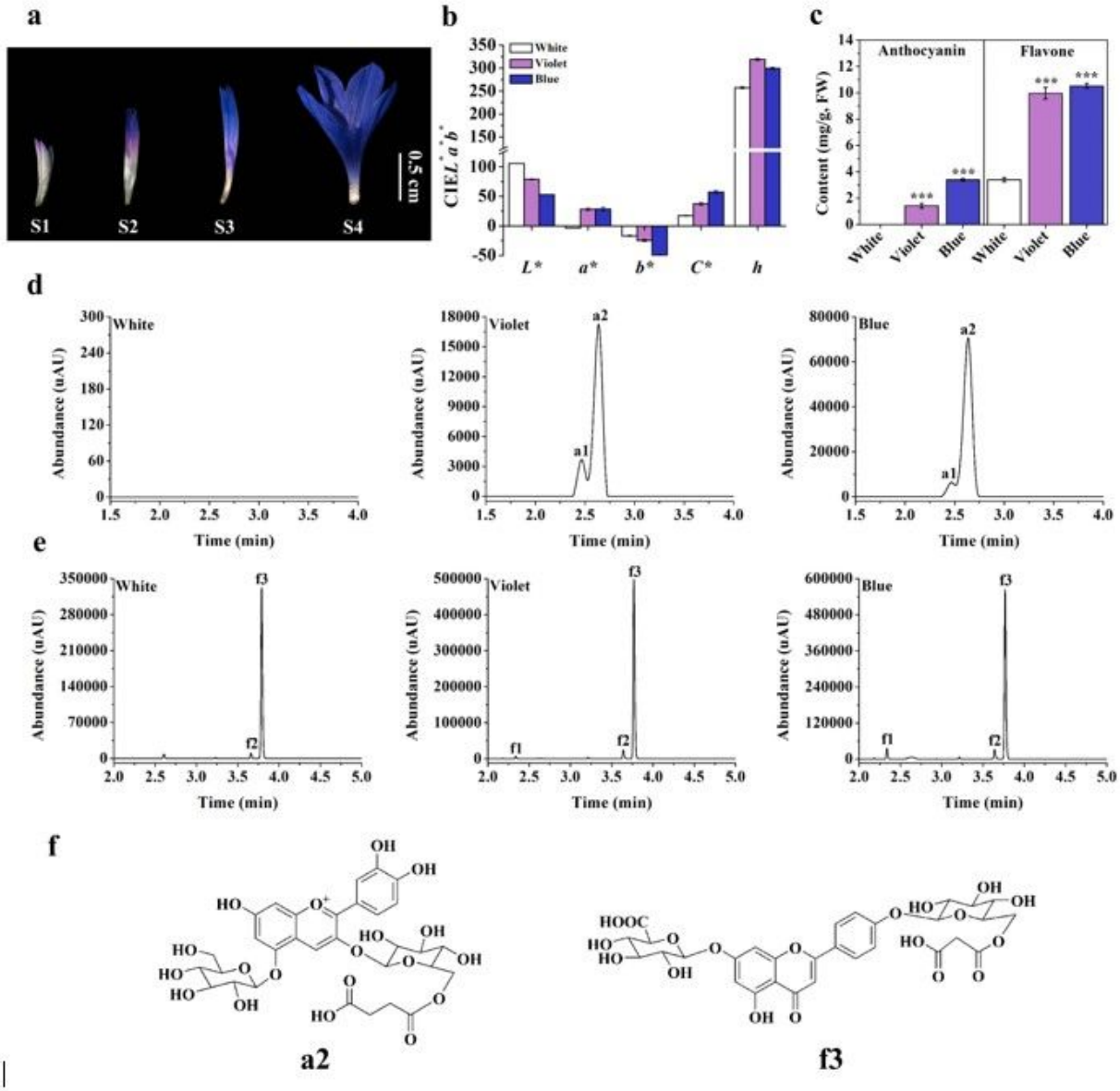

Fig. 1 The dynamic changes in phenotype and flavonoids during petal colour development in blue cornflower.

Figure 1

The dynamic changes in phenotype and flavonoids during petal colour development in blue cornflower.

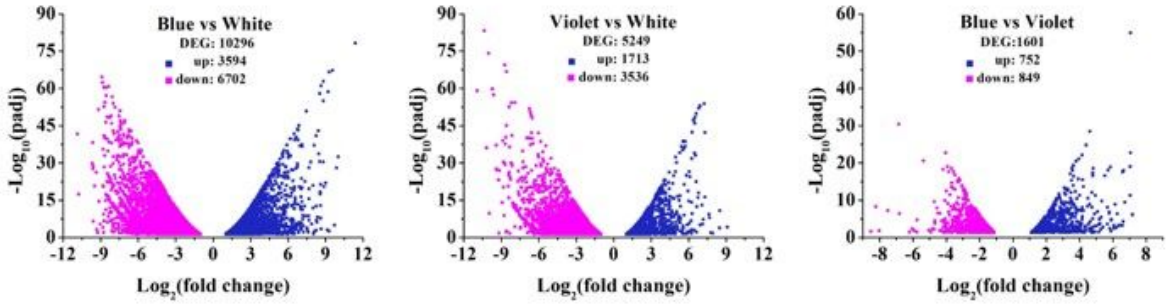

Fig. 2 Volcano plots of the transcriptome among three colour regions on the same petal.

Figure 2

Volcano plots of the transcriptome among three colour regions on the same petal.

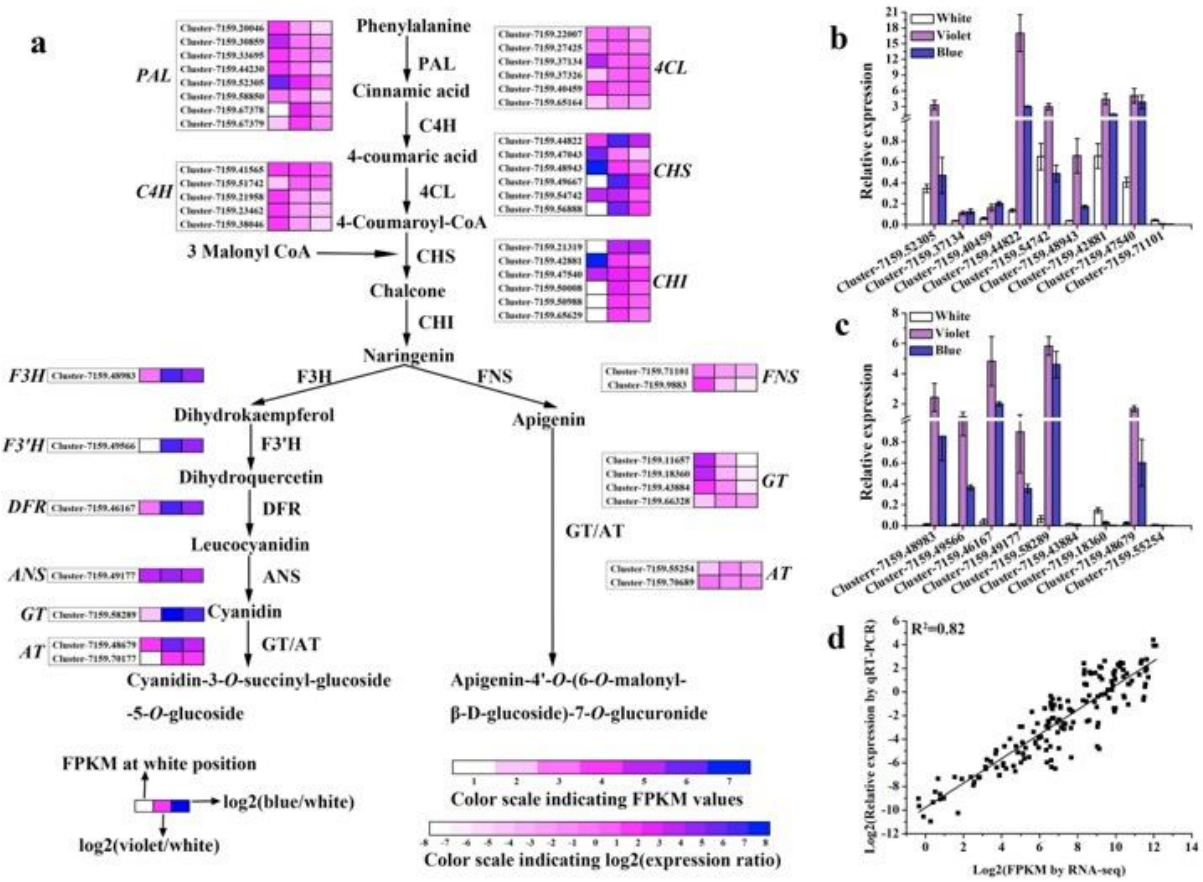

Fig. 3 Metabolite and gene expression involved in flavonoid biosynthesis in cornflower.

Figure 3

Metabolite and gene expression involved in flavonoid biosynthesis in cornflower.

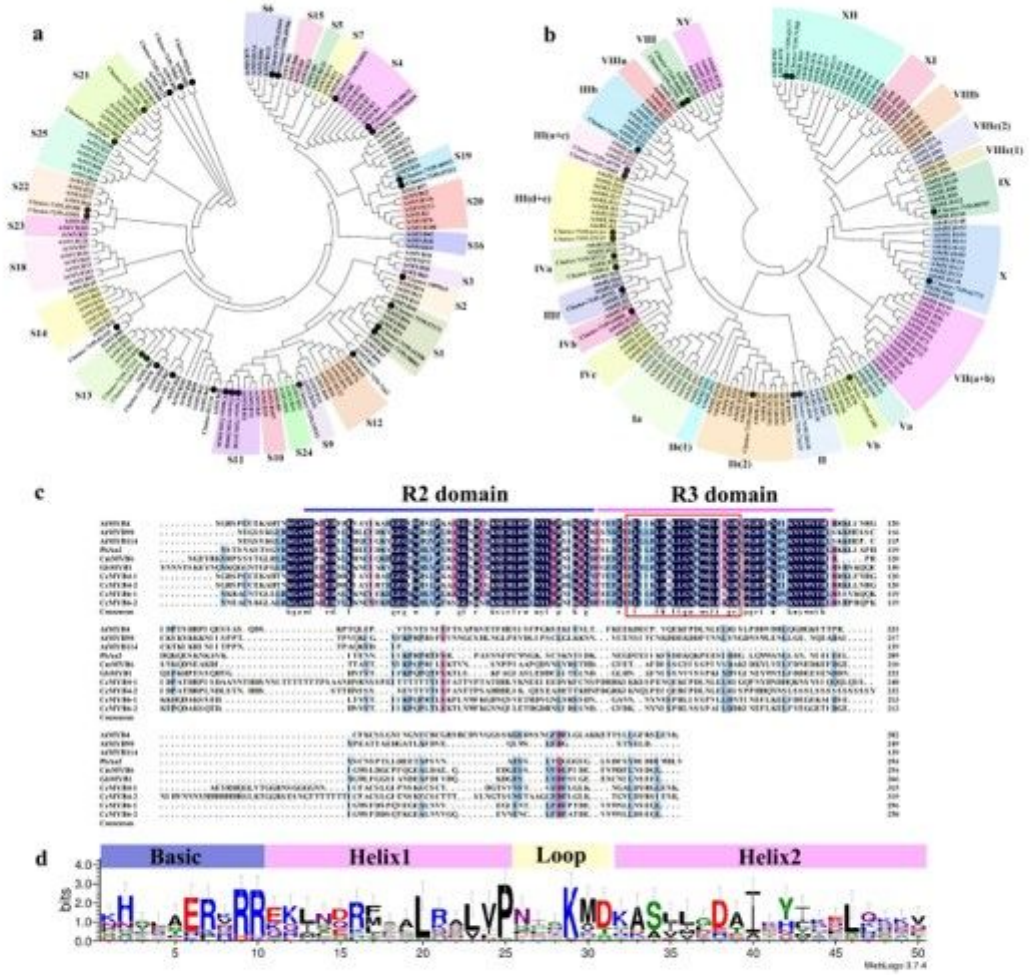

Fig. 4 The excavation of TFs involved in flavonoid biosynthesis.

Figure 4

The excavation of TFs involved in flavonoid biosynthesis.

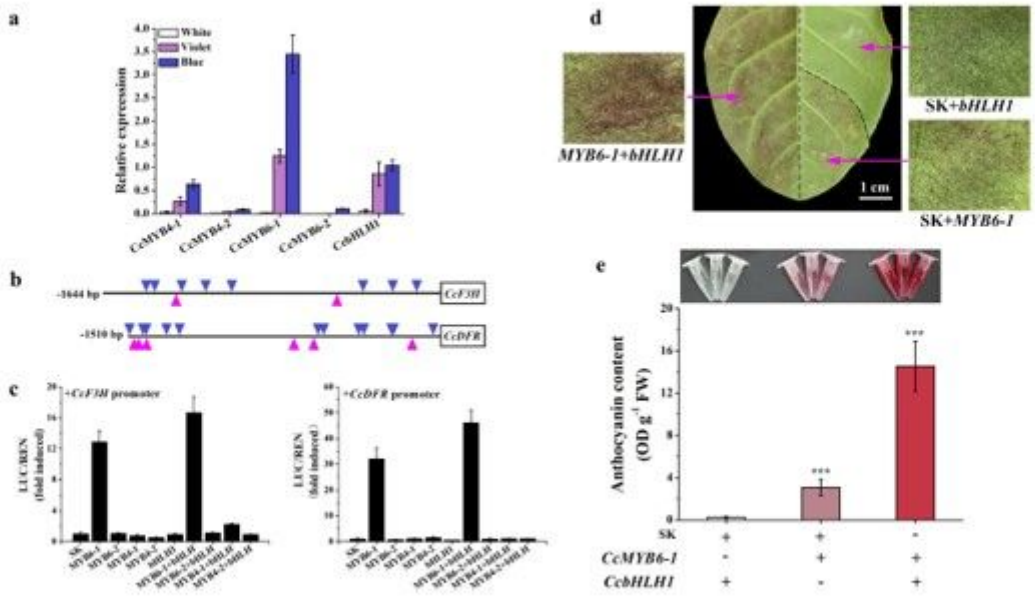

Fig. 5 Identification of TFs involved in anthocyanin biosynthesis.

Figure 5

Identification of TFs involved in anthocyanin biosynthesis.

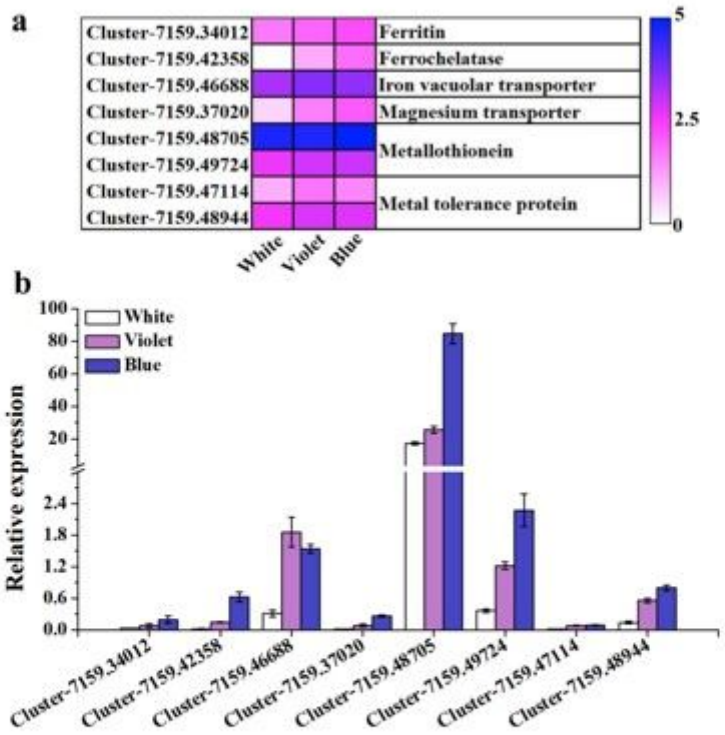

Fig. 6 Metal ion related genes with different expressions in the three colour regions on the same petal in cornflower.

Figure 6

Metal ion related genes with different expressions in the three colour regions on the same petal in cornflower.

Supplementary Files

This is a list of supplementary files associated with this preprint. Click to download.

- Additionalfile4.xlsx
- Additionalfile6.xlsx
- Additionalfile9.xlsx
- Additionalfile10.xlsx
- additionalfile2.docx
- CONSORT2010Checklist.doc
- Additionalfile8.xlsx
- Additionalfile7.docx
- Additionalfile3.docx

- additionalfile1.docx
- Additionalfile5.xlsx
- Additionalfile1.xlsx
- Additionalfile2.xlsx